# Electronic Supplementary Information

## Experimental

### *Materials*

Carbon cloth (CC) was used as the substrate. Cobalt nitrate hexahydrate ($Co(NO_3)_2 \cdot 6H_2O$, ≥ 99%) and sodium sulfide ($Na_2S \cdot 9H_2O$, ≥ 98%) were obtained from Aladdin Industrial Corporation. 2-Methylimidazole ($C_4H_6N_2$, ≥ 99.0%) was received from Sinopharm Chemical Reagent Co. Ltd. All chemicals employed were analytical grade. Experimental water was deionized water.

### *Synthesis of Co-MOF Nanoflakes Array on CC*

At first, the bare CC was pretreated by immersing in concentrated nitric acid and maintaining at 100 °C for 3 h in a Teflon-lined stainless steel autoclave. Co-MOF NF/CC was synthesized by a simple precipitation method. Specifically, 0.582 g of $Co(NO_3)_2 \cdot 6H_2O$ and 1.312 g of 2-methylimidazole ($C_4H_6N_2$) were dissolved respectively in 40 mL of deionized water to form solution A and solution B. After the solution B being rapidly added into the solution A to form a homogeneous suspension, a piece of pretreated CC substrate (2 × 3 $cm^2$) was quickly immersed in the above mixed solution. After reaction for 4 h at the room temperature, the material was taken out, cleaned with deionized water and dried at 60 °C overnight.

### *Synthesis of CoS Nanoflakes Array on CC*

Firstly, the $Co_3O_4$ NF/CC was obtained by annealing the prepared Co-MOF NF/CC in a tube furnace at 400 °C for 2 h with the heating rate of 2 °C $min^{-1}$ in air. Then, the preparation of CoS NF/CC was carried out through hydrothermal ion-exchange method. Concretely, 0.1 M $Na_2S \cdot 9H_2O$ aqueous solution served as reaction solution with a piece of obtained $Co_3O_4$ NF/CC as precursor. After reaction at 120 °C for 9 h and naturally cooled down to ambient temperature, the CoS NF/CC was synthesized, then washed thoroughly with water and dried at 60 °C in a vacuum environment. The loading masses of $Co_3O_4$ and CoS nanoflakes on CC are ~0.32 and ~0.72 mg $cm^{-2}$, respectively.

### *Synthesis of $RuO_2$*

$RuO_2$ powder was obtained in the light of a previously reported method. Specifically, 50 mL $RuCl_3 \cdot 3H_2O$ solution (0.1 M) and 15 mL KOH (1.0 M) were mixed and stirred gently at 100 °C for 45 min. Then, the precipitation was collected by centrifugation for 10 minutes at the rotation speed of 10000 r $min^{-1}$, and washed with deionized water for three times. Finally, the dried collection was annealed at 300 °C for 3 h in the air. Afterwards, 0.01 g of synthesized $RuO_2$ powder was dispersed in 0.5 mL ethanol/water/Nafion (v:v:v = 12:12:1) solution to form uniformly dispersed suspension with sonication for 30 min. Subsequently, 9 μL of the ink was dropped on CC (0.25 $cm^2$) and dried at room temperature.

***Physical characterization***

Scanning electron microscope (SEM), elemental mappings test and energy-dispersive spectrometry (EDS) were performed on Hitachi S-4800 operated at an accelerating voltage of 10 kV. Transmission electron microscopy (TEM), high-resolution TEM (HRTEM) and corresponding elemental mappings images were obtained by a Hitachi H-8100 electron microscopy (Hitachi, Tokyo, Japan) operated at 200 kV. X-ray diffraction (XRD) dates were gained from a Bruker D8 Advanced Diffractometer System with Cu Kα (1.5418 Å) as the radiation source (40 kV, 40 mA). X-ray photoelectron spectroscopy (XPS) measurements were taken on an ESCALABMK II X-ray photoelectron spectrometer using Mg as the exciting source. The BET analysis was performed with the $N_2$ adsorption/desorption isotherms at 77 K on a Micromeritics ASAP 2020 instrument.

***Electrochemical measurements***

Electrochemical measurements were conducted on a computer-controlled electrochemical workstation (CHI660E, CH Instruments, Inc., Shanghai) with a three-electrode configuration. The mercuric oxide electrode (MOE), graphite plate, and as-prepared catalytic materials acted as the reference electrode, counter electrode and working electrode, respectively. The area of working electrode is 0.25 $cm^2$ in all experiments. The electrocatalytic performance was evaluated by steady-state linear sweep voltammograms in 1.0 M KOH solution at a sweep rate of 2 mV $s^{-1}$. Measured voltage results were converted according to the equation: $E$ (RHE: reversible

hydrogen electrode) = $E$ (MOE) + 0.9254 V in 1.0 M KOH. The Tafel plots were obtained by overpotential ($\eta$) *vs.* log current (log |$j$|). The Tafel slope ($b$) was calculated by fitting the linear portion of the Tafel plots according to the Tafel equation [$\eta = b \log (j) + a$]. $iR$ corrected is on the basis of the equation: $E = E_m - iR_s$ (where $E$ is the corrected potential, $E_m$ is the measured potential, $i$ is the current density and $R_s$ is the resistance of the solution). The electrochemical double-layer capacitance ($C_{dl}$) was calculated by the equation of $C_{dl} = I/v$ from the CV curves in a potential range of 0.3−0.4 V without redox process, wherein $I$ is the charging current (mA $cm^{-2}$), and $v$ is the scan rate (mV $s^{-1}$). Electrochemical impedance spectroscopy (EIS) measurements were carried out by applying an AC voltage of 0.60 V with 5 mV amplitude in the frequency range from 100 kHz to 0.005 Hz. In addition, the obtained samples served as both the anode and the cathode to form a single-compartment cell to conduct overall water electrolysis with linear sweep voltammetry recorded in the voltage range from 2.0 V to 1.0 V. Multi-step and long-term chronopotentiometric measurements were employed to study the stability of catalysts.

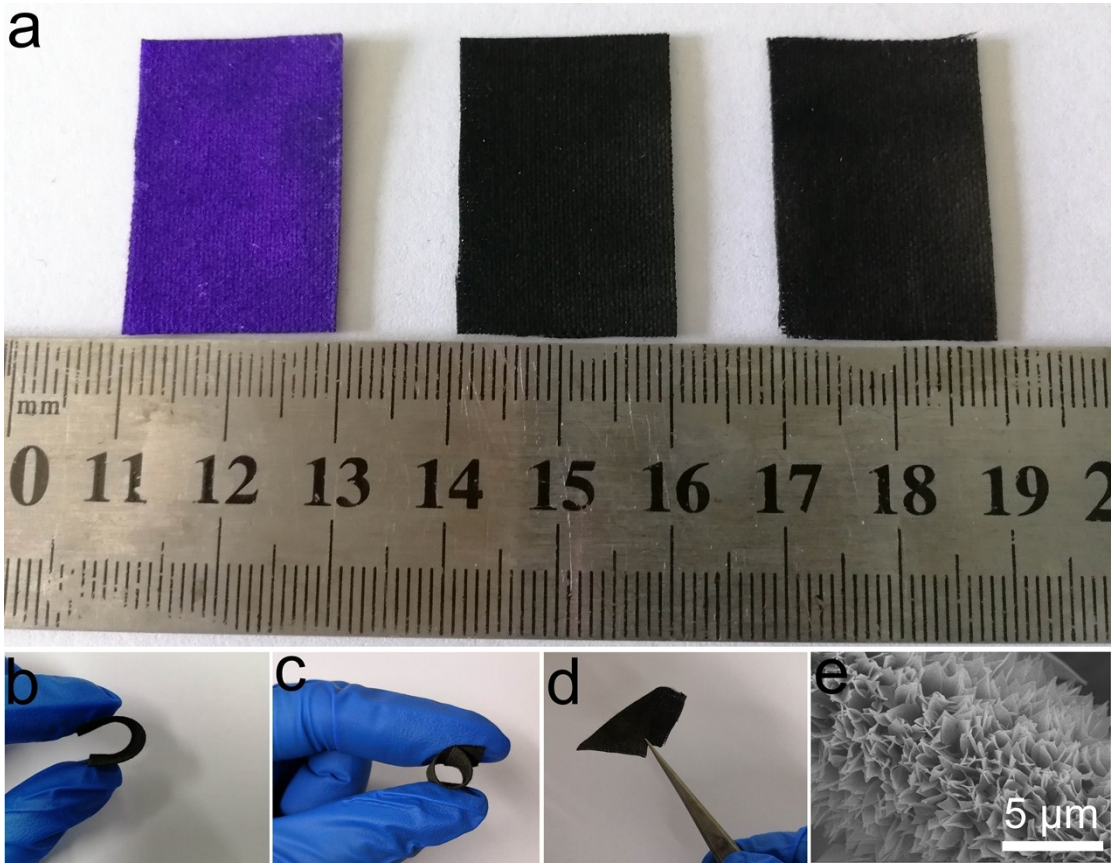


**Fig. S1.** (a) Optical image of Co-MOF NF/CC (left), $Co_3O_4$ NF/CC (middle), and CoS NF/CC (right). (b-d) Optical images of CoS NF/CC bended at different angles. (e) SEM image of CoS NF/CC after being bended at different angles.

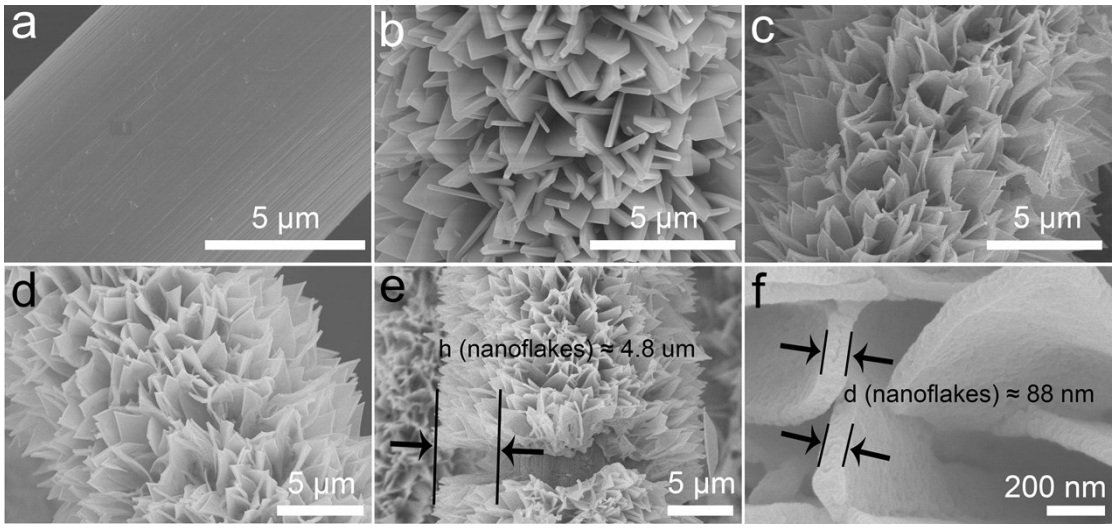


**Fig. S2.** SEM images of the (a) bare CC, (b) Co-MOF NF/CC, (c) $Co_3O_4$ NF/CC and (d) CoS NF/CC. (e) The height of CoS nanoflakes on CC. (f) The thickness of CoS nanoflakes.

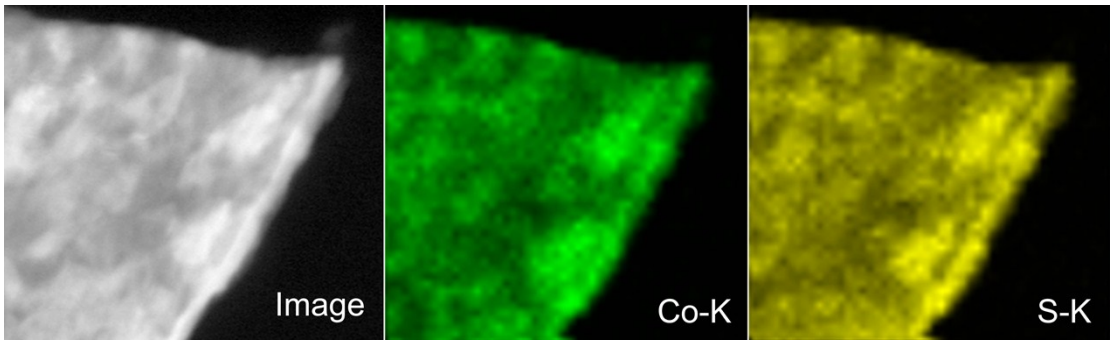

**Fig. S3.** Elemental mapping images for the CoS nanoflake.

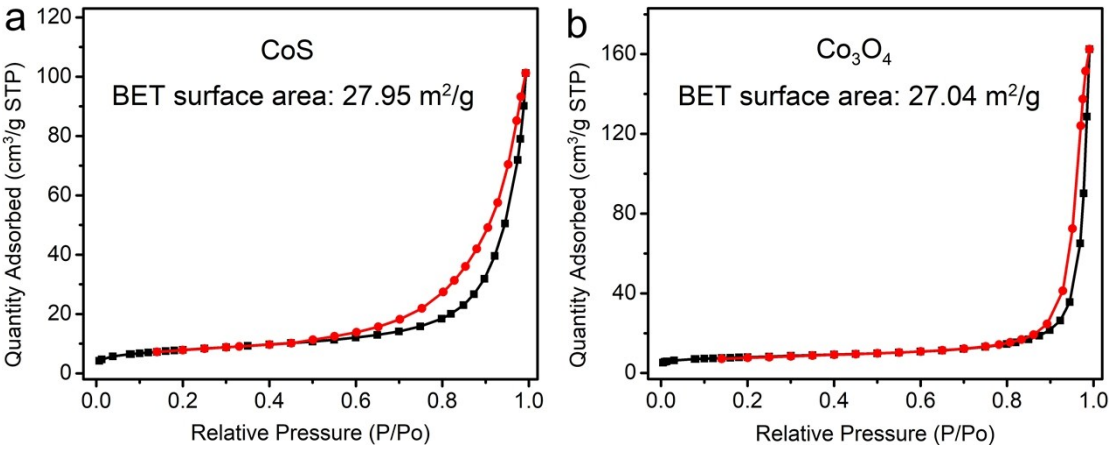


**Fig. S4.** $N_2$ adsorption/desorption isotherms obtained from the BET measurements of (a) CoS and (b) $Co_3O_4$ nanoflakes powders.

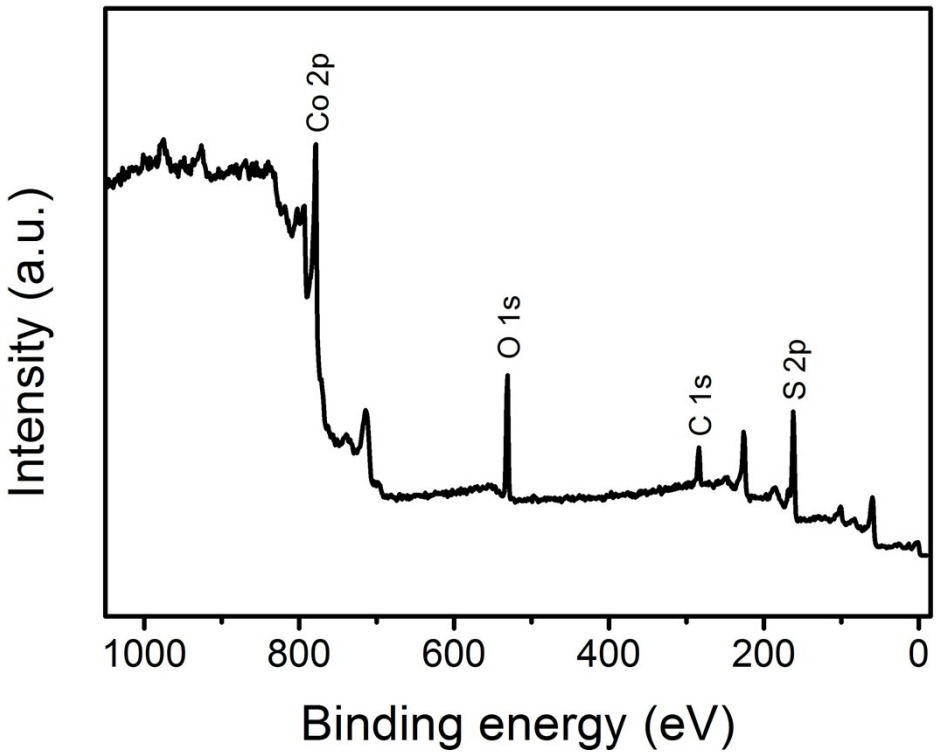


**Fig. S5.** XPS survey spectrum of CoS NF/CC.

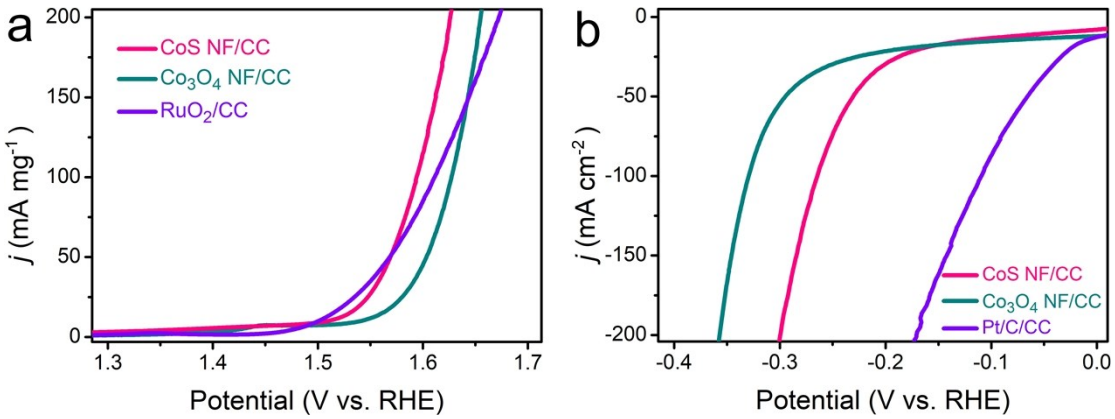


**Fig. S6.** (a) The mass-normalized OER performances of the CoS NF/CC, $Co_3O_4$ NF/CC and $RuO_2$/CC. (b) The mass-normalized HER performances of the CoS NF/CC, $Co_3O_4$ NF/CC and Pt/C/CC.

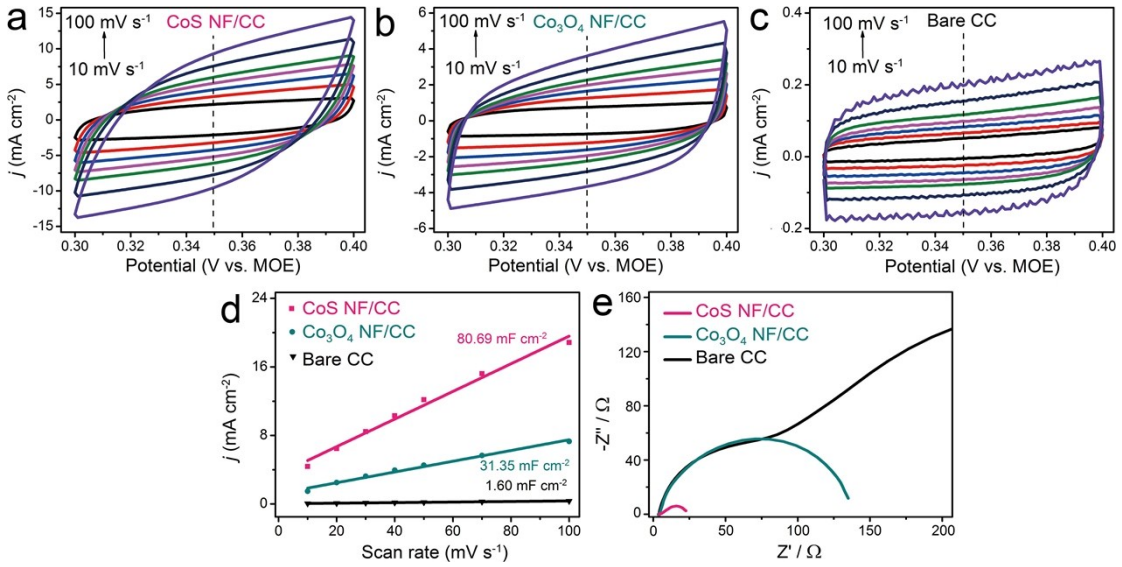


**Fig. S7.** Typical cyclic voltammograms of (a) CoS NF/CC, (b) $Co_3O_4$ NF/CC and (c) bare CC with various scan rates (10−100 mV $s^{-1}$) in the region of 0.3−0.4 V (*vs.* MOE). (d) The capacitive current density ($\Delta j$) at 0.35 V (*vs.* MOE) as a function of scan rate in the range of 0.3−0.4 V for different electrodes in 1.0 M KOH. (e) The Nyquist plots of CoS NF/CC, $Co_3O_4$ NF/CC and bare CC measured in 1.0 M KOH.

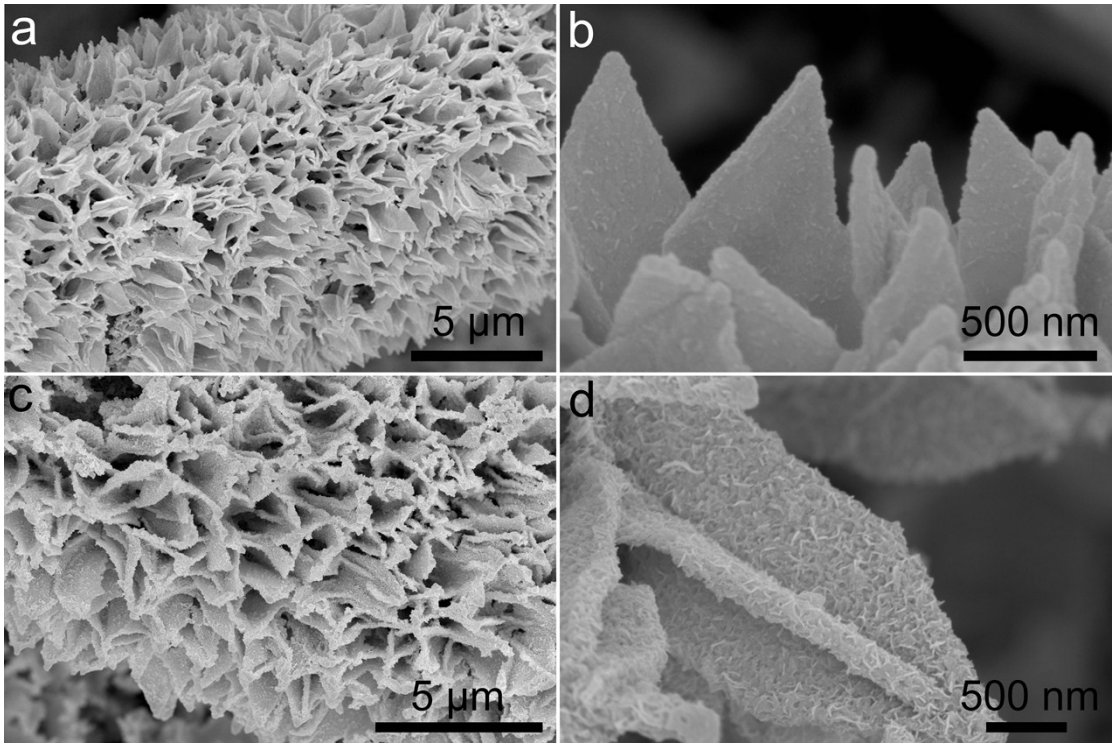


**Fig. S8.** SEM images of the CoS NF/CC after long-term (a,b) HER and (c,d) OER catalysis at 100 mA $cm^{-2}$.

**Table S1.** Comparison of the OER activity for the synthesized CoS NF/CC with several recently reported highly active electrocatalysts in alkaline solution.

| Catalytic material | Current density ($mA\ cm^{-2}$) | Overpotential (mV) | Ref. |
|---|---|---|---|
| **CoS NF/CC** | **10** | **310** | **This work** |
| Ni@CoO@CoNC | 10 | 309 | 1 |
| S,N-CNTs/$CoS_2$@Co | 10 | 340 | 2 |
| $NiCo_2S_4$ | 10 | 337 | 3 |
| $Ni_xCo_{3-x}O_4$ | 10 | 337 | 4 |
| $Co_9S_8$/N,S-CNS | 10 | 350 | 5 |
| $Co_9S_8$@$MoS_2$ | 10 | 342 | 6 |
| Au@$CoSe_2$ | 10 | 430 | 7 |
| NiO/Ni | 10 | 345 | 8 |
| β-$Ni(OH)_2$ | 10 | 340 | 9 |
| Co-$Cu_7S_4$-0.035 | 10 | 320 | 10 |
| $Fe_3O_4$@$Co_9S_8$/rGO-2 | 10 | 320 | 11 |
| NiCoS-3 polyhedron | 10 | 320 | 12 |
| $Zn_{0.1}Co_{0.9}Se_2$ | 10 | 340 | 13 |
| $Co_{1-x}S$@rGO | 10 | 310 | 14 |
| $Co_9S_8$@NOSC-900 | 10 | 330 | 15 |
| Mn-Co oxyphosphide | 10 | 320 | 16 |

**Table S2.** Comparison of the HER activity for the synthesized CoS NF/CC with several recently reported highly active electrocatalysts in alkaline solution.

| Catalytic material | Current density ($mA\ cm^{-2}$) | Overpotential (mV) | Ref. |
|---|---|---|---|
| **CoS NF/CC** | **50** | **247** | **This work** |
| Ni@CoO@CoNC | 50 | ~280 | 1 |
| $CoNi_2Se_4$@Au/glass | 50 | ＞300 | 17 |
| $Ni_3S_2$-NGQDs/NF | 50 | ~305 | 18 |
| $Ni_3Se_2$ nanoforest/NF | 50 | ~247 | 19 |
| $Ni_3S_2$ particles | 10 | 335 | 20 |
| Ni/NC | 20 | ~249 | 21 |
| Co/N-doped carbon | 10 | 260 | 22 |
| Co-S/CP | 10 | 357 | 23 |
| CP/CTs/Co-S | 30 | ~258 | |
| CoP nanowire array | 50 | ~375 | 24 |
| $Ni_3S_2$/NF | 20 | ~290 | 25 |
| $CoO_x$@CN | 20 | ~280 | 26 |
| CoSe/NiFe LDH | 10 | 260 | 27 |
| NiO/NF | 30 | ~255 | 28 |

**Table S3.** Comparison of the electrocatalysis activity for overall water splitting of the synthesized CoS NF/CC with several recently reported highly active electrocatalysts in alkaline solution.

| Catalytic material | Current density ($mA\ cm^{-2}$) | Voltage (V) | Ref. |
|---|---|---|---|
| **CoS NF/CC** | **10** | **1.72** | **This work** |
| $Ni_xCo_{3-x}O_4$/NiCo/$NiCoO_x$ | 10 | 1.75 | 4 |
| Co-P/NC/CC | 10 | 1.77 | 14 |
| CP/CTs/Co-S | 10 | 1.74 | 23 |
| amorphous $Co_2B$ | 10 | 1.81 | 29 |
| $Ni_{0.85}Se$/GS | 10 | 1.73 | 30 |
| V/NF | 10 | 1.74 | 31 |
| $Co_3O_4$ | 10 | 1.91 | 32 |
| $Mo_2C$@CS | 10 | 1.73 | 33 |
| CoO/$MoO_X$ | 10 | 1.72 | 34 |
| $Ni(OH)_2$/$NiSe_2$ | 10 | 1.78 | 35 |
| $NiCo_2O_4$\|\|$Ni_{0.33}Co_{0.67}S_2$/Ti foil | 10 | 1.72 | 36 |
| NiSe/Ni | 20 | 1.75 | 37 |
| $Ni_3S_2$ on nickel foam | 10 | 1.73 | 38 |
| NiCo-LDH | 10 | 1.73 | 39 |
| $NiCo_2S_4$ nanowires array | 20 | 1.85 | 40 |

**Reference**

[1] G. Cai, W. Zhang, L. Jiao, S.-H. Yu and H.-L. Jiang, Template-directed growth of well-aligned MOF arrays and derived self-supporting electrodes for water splitting. *Chem*, 2017, **2**, 791-802.

[2] J.-Y. Wang, T. Ouyang, N. Li, T. Ma and Z.-Q. Liu, S,N co-doped carbon nanotube-encapsulated core-shelled $CoS_2$@Co nanoparticles: efficient and stable bifunctional catalysts for overall water splitting. *Sci. Bull*., 2018, **63**, 1130-1140.

[3] J. Jiang, C. Yan, X. Zhao, H. Luo, Z. Xue and T. Mu, A PEGylated deep eutectic solvent for controllable solvothermal synthesis of porous $NiCo_2S_4$ for efficient oxygen evolution reaction. *Green Chem*., 2017, **19**, 3023-3031.

[4] X. Yan, K. Li, L. Lyu, F. Song, J. He, D. Niu, L. Liu, X. Hu and X. Chen, From water oxidation to reduction: transformation from $Ni_xCo_{3-x}O_4$ nanowires to NiCo/$NiCoO_x$ heterostructures. *ACS Appl. Mater. Interfaces*, 2016, **8**, 3208-3214.

[5] C. Wu, Y. Zhang, D. Dong, H. Xie and J. Li, $Co_9S_8$ nanoparticles anchored on nitrogen and sulfur dual-doped carbon nanosheets as highly efficient bifunctional electrocatalyst for oxygen evolution and reduction reactions. *Nanoscale*, 2017, **9**, 12432-12440.

[6] J. Bai, T. Meng, D. Guo, S. Wang, B. Mao and M. Cao, $Co_9S_8$@$MoS_2$ core-shell heterostructures as trifunctional electrocatalysts for overall water splitting and Zn-air batteries. *ACS Appl. Mater. Interfaces*, 2018, **10**, 1678-1689.

[7] S. Zhao, R. Jin, H. Abroshan, C. Zeng, H. Zhang, S. D. House, E. Gottlieb, H. J. Kim, J. C. Yang and R. Jin, Gold nanoclusters promote electrocatalytic water oxidation at the nanocluster/$CoSe_2$ interface. *J. Am. Chem. Soc.*, 2017, **139**, 1077-1080.

[8] J. Liang, Y.-Z. Wang, C.-C. Wang and S.-Y. Lu, *In situ* formation of NiO on Ni foam prepared with a novel leaven dough method as an outstanding electrocatalyst for oxygen evolution reactions. *J. Mater. Chem. A*, 2016, **4**, 9797-9806.

[9] S. C. Jung, S. L. Sim, Y. W. Soon, C. M. Lim, P. Hing and J. R. Jennings, Synthesis of nanostructured β-$Ni(OH)_2$ by electrochemical dissolution-precipitation and its application as a water oxidation catalyst. *Nanotechnology*, 2016, **27**, 275401.

[10] Q. Li, X. Wang, K. Tang, M. Wang, C. Wang and C. Yan, Electronic modulation of electrocatalytically active center of $Cu_7S_4$ nanodisks by cobalt-doping for highly efficient oxygen evolution reaction. *ACS Nano*, 2017, **11**, 12230-12239.

[11] M. Gao, W. Sheng, Z. Zhuang, Q. Fang, S. Gu, J. Jiang and Y. Yan, Efficient water oxidation using nanostructured α-nickel-hydroxide as an electrocatalyst. *J. Am. Chem. Soc*., 2014, **136**, 7077-7084.

[12] Z. Yu, Y. Bai, S. Zhang, Y. Liu, N. Zhang and K. Sun, MOF-directed templating synthesis of hollow nickel-cobalt sulfide with enhanced electrocatalytic activity for

oxygen evolution. *Int. J. Hydrogen Energ*., 2018, **43**, 8815-8823.
[13] X. Wang, F. Li, W. Li, W. Gao, Y. Tang and R. Li, Hollow bimetallic cobalt-based selenide polyhedrons derived from metal-organic framework: an efficient bifunctional electrocatalyst for overall water splitting. *J. Mater. Chem. A*, 2017, **5**, 17982-17989.
[14] J. Q. Zhu, Z. Y. Ren, S. C. Du, Y. Xie, J. Wu, H. Y. Meng, Y. Z. Xue and H. G. Fu, Co-vacancy-rich $Co_{1-x}S$ nanosheets anchored on rGO for high-efficiency oxygen evolution. *Nano Res*., 2017, **10**, 1819-1831.
[15] S. Huang, Y. Meng, S. He, A. Goswami, Q. Wu, J. Li, S. Tong, T. Asefa and M. Wu, N-, O-, and S-tridoped carbon-encapsulated $Co_9S_8$ nanomaterials: efficient bifunctional electrocatalysts for overall water splitting. *Adv. Funct. Mater*., 2017, **27**, 1606585.
[16] B. Y. Guan, L. Yu and X. W. Lou, General synthesis of multishell mixed-metal oxyphosphide particles with enhanced electrocatalytic activity in the oxygen evolution reaction. *Angew. Chem. Int. Ed*., 2017, **56**, 2386-2389.
[17] B. G. Amin, A. T. Swesi, J. Masud and M. Nath, $CoNi_2Se_4$ as an efficient bifunctional electrocatalyst for overall water splitting. *Chem. Commun.*, 2017, **53**, 5412-5415.
[18] J.-J. Lv, J. Zhao, H. Fang, L.-P. Jiang, L.-L. Li, J. Ma and J.-J. Zhu, Incorporating nitrogen-doped graphene quantum dots and $Ni_3S_2$ nanosheets: a synergistic electrocatalyst with highly enhanced activity for overall water splitting. *Small*, 2017, **13**, 1700264.
[19] R. Xu, R. Wu, Y. Shi, J. Zhang and B. Zhang, $Ni_3Se_2$ nanoforest/Ni foam as a hydrophilic, metallic, and self-supported bifunctional electrocatalyst for both $H_2$ and $O_2$ generations. *Nano Energy*, 2016, **24**, 103-110.
[20] N. Jiang, Q. Tang, M. Sheng, B. You, D.-E. Jiang and Y. Sun, Nickel sulfides for electrocatalytic hydrogen evolution under alkaline conditions: a case study of crystalline NiS, $NiS_2$, and $Ni_3S_2$ nanoparticles. *Catal. Sci. Technol*., 2016, **6**, 1077-1084.
[21] X. Zhang, H. Xu, X. Li, Y. Li, T. Yang and Y. Liang, Facile synthesis of nickel-iron/nanocarbon hybrids as advanced electrocatalysts for efficient water splitting. *ACS Catal*., 2016, **6**, 580-588.
[22] H. Zhang, Z. Ma, J. Duan, H. Liu, G. Liu, T. Wang, K. Chang, M. Li, L. Shi, X. Meng, K. Wu and J. Ye, Active sites implanted carbon cages in core-shell architecture: highly active and durable electrocatalyst for hydrogen evolution reaction. *ACS Nano*, 2016, **10**, 684-694.
[23] J. Wang, H. Zhong, Z. Wang F. Meng and X. Zhang, Integrated three-dimensional carbon paper/carbon tubes/cobalt-sulfide sheets as an efficient electrode for overall water splitting. *ACS Nano*, 2016, **10**, 2342-2348.

[24] J. Tian, Q. Liu, A. M. Asiri and X. Sun, Self-supported nanoporous cobalt phosphide nanowire arrays: an efficient 3D hydrogen-evolving cathode over the wide range of pH 0–14. *J. Am. Chem. Soc*., 2014, **136**, 7587-7590.
[25] L.-L. Feng, G. Yu, Y. Wu, G.-D. Li, H. Li, Y. Sun, T. Asefa, W. Chen and X. Zou, High-index faceted $Ni_3S_2$ nanosheet arrays as highly active and ultrastable electrocatalysts for water splitting. *J. Am. Chem. Soc*., 2015, **137**, 14023-14026.
[26] H. Jin, J. Wang, D. Su, Z. Wei, Z. Pang and Y. Wang, *In situ* cobalt-cobalt oxide/N-doped carbon hybrids as superior bifunctional electrocatalysts for hydrogen and oxygen evolution. *J. Am. Chem. Soc*., 2015, **137**, 2688-2694.
[27] Y. Hou, M. R. Lohe, J. Zhang, S. Liu, X. Zhuang and X. Feng, Vertically oriented cobalt selenide/NiFe layered-double-hydroxide nanosheets supported on exfoliated graphene foil: an efficient 3D electrode for overall water splitting. *Energy Environ. Sci*., 2016, ***9***, 478-483.
[28] J. Liu, Y. Zheng, Y. Jiao, Z. Wang, Z. Lu, A. Vasileff and S.-Z. Qiao, NiO as a bifunctional promoter for $RuO_2$ toward superior overall water splitting. *Small*, 2018, **14**, 1704073.
[29] J. Masa, P. Weide, D. Peeters, I. Sinev, W. Xia, Z. Sun, C. Somsen, M. Muhler and W. Schuhmann, Amorphous cobalt boride ($Co_2B$) as a highly efficient nonprecious catalyst for electrochemical water splitting: oxygen and hydrogen evolution. *Adv. Energy Mater*., 2016, **6**, 1502313.
[30] X. Wu, D. He, H. Zhang, H. Li, Z. Li, B. Yang, Z. Lin, L. Lei and X. Zhang, $Ni_{0.85}Se$ as an efficient non-noble bifunctional electrocatalyst for full water splitting. *Int. J. Hydrogen Energy*, 2016, **41**, 10688-10694.
[31] Y. Yu, P. Li, X. Wang, W. Gao, Z. Shen, Y. Zhu, S. Yang, W. Song and K. Ding, Vanadium nanobelts coated nickel foam 3D bifunctional electrode with excellent catalytic activity and stability for water electrolysis. *Nanoscale*, 2016, **8**, 10731-10738.
[32] S. Du, Z. Ren, J. Zhang, J. Wu, W. Xi, J. Zhu and H. Fu, $Co_3O_4$ nanocrystal ink printed on carbon fiber paper as a large-area electrode for electrochemical water splitting. *Chem. Commun.*, 2015, **51**, 8066-8069.
[33] H. Wang, Y. Cao, C. Sun, G. Zou, J. Huang, X. Kuai, J. Zhao and L. Gao, Strongly coupled molybdenum carbide on carbon sheets as a bifunctional electrocatalyst for overall water splitting. *ChemSusChem*, 2017, **10**, 3540-3546.
[34] X. Yan, L. Tian, S. Atkins, Y. Liu, J. Murowchick and X. Chen, Converting $CoMoO_4$ into $CoO/MoO_x$ for overall water splitting by hydrogenation. *ACS Sustainable Chem. Eng*., 2016, **4**, 3743-3749.
[35] H. Liang, L. Li, F. Meng, L. Dang, J. Zhuo, A. Forticaux, Z. Wang and S. Jin, Porous two-dimensional nanosheets converted from layered double hydroxides and their applications in electrocatalytic water splitting. *Chem. Mater.*, 2015, **27**, 5702-5711.

[36] Z. Peng, D. Jia, A. M. Al-Enizi, A. A. Elzatahry and G. Zheng, From water oxidation to reduction: homologous Ni-Co based nanowires as complementary water splitting electrocatalysts. *Adv. Energy Mater*., 2015, **5**, 1402031.
[37] C. Tang, N. Cheng, Z. Pu, W. Xing, X. Sun, NiSe nanowire film supported on nickel foam: an efficient and stable 3D bifunctional electrode for full water splitting. *Angew. Chem. Int. Ed.*, 2015, **54**, 9351-9355.
[38] A. Sivanantham, P. Ganesan and S. Shanmugam, Hierarchical $NiCo_2S_4$ nanowire arrays supported on Ni foam: an efficient and durable bifunctional electrocatalyst for oxygen and hydrogen evolution reactions. *Adv Funct Mater*, 2016, **26**, 4661-4672.
[39] K. Xiao, L. Zhou, M. Shao and M. Wei, Fabrication of $(Ni,Co)_{0.85}Se$ nanosheet arrays derived from layered double hydroxides toward largely enhanced overall water splitting. *J. Mater. Chem. A*, 2018, **6**, 7585-7591.
[40] D. Liu, Q. Lu, Y. Luo, X. Sun and A. M. Asiri, $NiCo_2S_4$ nanowires array as an efficient bifunctional electrocatalyst for full water splitting with superior activity. *Nanoscale*, 2015, **7**, 15122-15126.